Available online at www.sciencedirect.com
SCIENCE DIRECT®
Journal of Inorganic Biochemistry 95 (2003) 270–282
JOURNAL OF Inorganic Biochemistry
www.elsevier.com/locate/jinorgbio

Coordination abilities of the 1–16 and 1–28 fragments of β-amyloid peptide towards copper(II) ions: a combined potentiometric and spectroscopic study

Teresa Kowalik-Jankowska[a,*], Monika Ruta[a], Kornelia Wiśniewska[b], Leszek Łankiewicz[b]

[a]*Faculty of Chemistry, University of Wrocław, Joliot-Curie 14, 50-383 Wrocław, Poland*
[b]*Faculty of Chemistry, University of Gdańsk, Sobieskiego 18, 80-952 Gdańsk, Poland*

Received 5 March 2003; received in revised form 9 April 2003; accepted 14 April 2003

Abstract

Stoichiometry, stability constants and solution structures of the copper(II) complexes of the (1–16**H**), (1–28**H**), (1–16**M**), (1–28**M**), (Ac-1–16**H**) and (Ac-1–16**M**) fragments of human (**H**) and mouse (**M**) β-amyloid peptide were determined in aqueous solution in the pH range 2.5–10.5. The potentiometric and spectroscopic data (UV–Vis, CD, EPR) show that acetylation of the amino terminal group induces significant changes in the coordination properties of the (Ac-1–16**H**) and (Ac-1–16**M**) peptides compared to the (1–16**H**) and (1–16**M**) fragments, respectively. The (Ac-1–16**H**) peptide forms the 3N $\{N^{6}_{Im}, N^{13}_{Im}, N^{14}_{Im}\}$ complex in a wide pH range (5–8), while for the (Ac-1–16**M**) fragment the 2N $\{N^{6}_{Im}, N^{14}_{Im}\}$ complex in the pH range 5–7 is suggested. At higher pH values sequential amide nitrogens are deprotonated and coordinated to copper(II) ions. The N-terminal amino group of the (1–16) and (1–28) fragments of human and mouse β-amyloid peptide takes part in the coordination of the metal ion, although, at pH above 9 the complexes with the 4N $\{N_{Im}, 3N^{-}\}$ coordination mode are formed. The phenolate –OH group of the Tyr^{10} residue of the human fragments does not coordinate to the metal ion.

Keywords: β-Amyloid peptide fragments; Alzheimer's disease; Copper(II) complexes; Stability constants; Spectroscopic studies

1. Introduction

Patients with Alzheimer's disease (AD) contain large quantities of insoluble amyloid plaques that are primarily found in brain tissue. A major component of amyloid plaque is the β-peptide (Aβ) [1,2], a small (39–43 amino acids) polypeptide with heterogenous termini that is generated from the cleavage of a larger amyloid precursor protein (APP) [3,4]. Amyloid deposition is likely a critical step in the neurodegenerative processes associated with AD [5]. Amyloid plaques are invariably associated with areas of nerve death, and the injection of synthetic β-peptides directly into rat brain produced cytotoxic effects [6]. It has also recently been established that soluble extracellular β-peptide is normally produced in cultured cells and human biological fluids [7,8].

There is an emerging consensus in the literature to indicate that the homeostases of zinc, copper and iron are significantly altered in AD brain tissue [9]. Evidence for abnormal Cu homeostasis in AD includes a 2.2-fold increase in the concentration of cerebrospinal fluid (CSF) Cu [10], and an accompanying increase in ceruloplasmin in the brain and CSF of AD patients [11]. Aβ is resolubilized and extracted from postmortem AD and non-AD control brains using metal chelators. High-affinity Cu/Zn/Fe chelators markedly enhanced the resolubilization of AD deposits from postmortem AD and non-AD brain samples [12]. Aβ in vitro binds metal ions, including Zn^{2+}, Cu^{2+}, and Fe^{3+}, inducing peptide aggregation that may be reversed by treatment with chelators such as ethylenediaminetetraacetic acid (EDTA) [13,14]. Rats and mice do not develop amyloid [15], probably due to the three amino acid substitutions in their homologue of Aβ (Arg^{5}→Gly, Tyr^{10}→Phe, and His^{13}→Arg) [16]. These changes have been shown to alter the structure and properties of the Aβ peptides [17–19] as well as the processing of APP. These sequence alternations might therefore be responsible for

*Corresponding author. Tel.: +48-71-375-7231; fax: +48-71-328-2348.
E-mail address: terkow@wchuwr.chem.uni.wroc.pl (T. Kowalik-Jankowska).

0162-0134/03/$ – see front matter
doi:10.1016/S0162-0134(03)00128-4

the virtual absence of Aβ deposits in normal or aged rodent brain [19]. In vitro it has been shown that, compared with human Aβ, rat Aβ binds Zn^{2+} and Cu^{2+} less avidly [13], that the coordination of Cu^{2+} or Fe^{3+} does not induce redox chemical reactions, and that limited reactive oxygen species are generated [20]. Through the use of synthetic peptide corresponding to the first 28 residues of human Aβ, rat Aβ, and single-residue variations, Liu et al. [21] reported a key role for His^{13} in the zinc interaction. Substitution His/Ala of the potential histidine ligands in Aβ suggests that residues His^{13} and His^{14} represent a critical domain for zinc interaction [22]. On the basis of nuclear magnetic resonance (NMR) and electron paramagnetic resonance (EPR) experiments, it has been proposed that Aβ binds Cu^{2+} via three His residues (His^{6}, His^{13} and His^{14}) and an oxygen ligand, probably Tyr^{10} [23].

Peptide complexes with metal ions have been extensively studied in order to mimic specific metalloprotein structures and functions [24,25]. A prominent role of some amino acid side chains and, in particular, the imidazole moieties of histidine in the binding of metal ion has been observed in proteins and in natural [26] or synthetic peptides [27,28]. The studies of metal ion–peptide complex formation reactions indicate that solution equilibria are rather complicated especially in the presence of coordinating side chains. For the determination of formation constants of peptide complexes potentiometry is usually used, but for the justification of potentiometric results the combined application of various spectroscopic techniques: UV–visible (UV–Vis), EPR, NMR and/or circular dichroism (CD) spectroscopies is required.

The interaction of copper(II) ions with the (1–6), (1–9), (1–10) [29] (contain one His^{6} residue) and (11–16) [30], (11–20), (11–28) [31] human (contain two His^{13} and His^{14} residues) and mouse (one His^{14} residue) fragments of β-amyloid peptide was studied. The differences of the binding mode of human and mouse fragments to copper(II) ions and stability constants for the complexes formed were determined.

The present paper reports the results of combined spectroscopic and potentiometric studies on the copper(II) complexes of the (1–16) and (1–28) human (three His^{6}, His^{13}, His^{14} residues) and mouse (two His^{6}, His^{14} residues) fragments of β-amyloid peptide. The β-amyloid fragments studied here are: human peptide (1–16**H**), H-Asp–Ala–Glu–Phe–Arg–His–Asp–Ser–Gly–Tyr–Glu–Val–His–His–Gln–Lys-NH_2, DAEFRHDSGYEVHHQK-NH_2 and mouse peptide (1–16**M**), H-Asp–Ala–Glu–Phe–Gly–His–Asp–Ser–Gly–Phe–Glu–Val–Arg–His–Gln–Lys-NH_2, DAEFGHDSGFEVRHQK-NH_2; the fragments (1–28), human peptide (1–28**H**), H-Asp–Ala–Glu–Phe–Arg–His–Asp–Ser–Gly–Tyr–Glu–Val–His–His–Gln–Lys–Leu–Val–Phe–Phe–Ala–Glu–Asp–Val–Gly–Ser–Asn–Lys-NH_2, DAEFRHDSGYEVHHQKLVFFAEDVGSNK-NH_2 and mouse peptide (1–28**M**) H-Asp–Ala–Glu–Phe–Gly–His–Asp–Ser–Gly–Phe–Glu–Val–Arg–His–Gln–Lys–Leu–Val–Phe–Phe–Ala–Glu–Asp–Val–Gly–Ser–Asn–Lys-NH_2, DAEFGHDSGFEVRHQKLVFFAEDVGSNK-NH_2. To determine the involvement of N-terminal amino group in the metal ion coordination, the analogues with blocked N-terminal amino group (by acetylation) of the human and mouse fragments (1–16): human (Ac-1–16**H**), Ac-Asp–Ala–Glu–Phe–Arg–His–Asp–Ser–Gly–Tyr–Glu–Val–His–His–Gln–Lys-NH_2, Ac-DAEFRHDSGYEVHHQK-NH_2; mouse (Ac-1–16**M**), Ac-Asp–Ala–Glu–Phe–Gly–His–Asp–Ser–Gly–Phe–Glu–Val–Arg–His–Gln–Lys-NH_2, Ac-DAEFGHDSGFEVRHQK-NH_2 were also studied. These fragments contain the complete bonding site of Aβ and, with the exception of the C-terminal carboxylate, are representative of the full-length peptide. Therefore, the 1–16 and 1–28 fragments are considered as valid models to examine the contribution of the key histidine residues (His^{6}, His^{14} in mouse and His^{6}, His^{13}, His^{14} in human fragments) to the Aβ–Cu^{2+} interaction. This study was performed in order to examine the difference of the binding ability of the human and mouse fragments, especially the effect of the substitutions Arg with Gly, Tyr with Phe and His with Arg residues in positions 5, 10 and 13, respectively, on the formation of complexes with Cu^{2+} ions. The (17–28) fragment of β-amyloid peptide does not contain any additional bonding site to copper(II) ions, however, the influence of these residues on the stability of the complexes formed may be estimated.

2. Experimental

2.1. Peptide synthesis, purification and characterization

Syntheses of peptide amides: fragments of human (**H**) and mouse (**M**) β-amyloid peptide (Aβ): (1–16**H**), (1–16**M**), (Ac-1–16**H**), (Ac-1–16**M**), (1–28**H**) and (1–28**M**) were synthesized by solid phase methodology and purified according to the procedure described earlier [29].

The purity of the peptides was assessed by reversed-phase high-performance liquid chromatography (RP-HPLC) [29] and fast atom bombardment mass spectrometry (FAB-MS) or matrix-assisted laser desorption/ionization (MALDI). Purity of all the peptides was also checked by potentiometry.

Analytical data were as follows: 1–16**H**—R_t(HPLC)=20.77 min, M^++1(FAB-MS)=1955; 1–16**M**—R_t(HPLC)=21.35 min, M^++1(FAB-MS)=1859; Ac-1–16**H**—R_t(HPLC)=21.65 min, M^++1(FAB-MS)=1997; Ac-1–16**M**—R_t(HPLC)=22.62 min, M^++1(FAB-MS)=1901; 1–28**H**—R_t(HPLC)=27.73 min, M^++1(MALDI-TOF)=3262.5; 1–28**M**—R_t(HPLC)=27.99 min, M^++1(MALDI-TOF)=3165.5.

2.2. Potentiometric measurements

Stability constants for proton and Cu^{2+} complexes were

calculated from pH-metric titrations carried out in argon atmosphere at 298 K using a total volume of 2–3 cm^3. Alkali was added from a 0.250 cm^3 micrometer syringe which was calibrated by both weight titration and the titration of standard materials. Experimental details: ligand concentration $3–6\times10^{-4}$ mol dm^{-3}; metal-to-ligand molar ratio 1:1.1; ionic strength 0.10 mol dm^{-3} (KNO_3); $Cu(NO_3)_2$ was used as the source of the metal ions; pH-metric titration on a MOLSPIN pH-meter system using a Russel CMAW 711 semi-micro combined electrode, calibrated in concentration using HNO_3 [32], number of titrations, two; method of calculation SUPERQUAD [33]. The samples were titrated in the pH region 2.5–10.5. Standard deviations (σ values) quoted were computed by SUPERQUAD and refer to random errors only. They are, however, a good indication of the importance of the particular species involved in the equilibria.

2.3. Spectroscopic measurements

Absorption spectra were recorded on a Beckman DU 650 spectrophotometer. Circular dichroism (CD) spectra were recorded on a Jasco J-715 spectropolarimeter in the 750–260 nm range. The values of $\Delta\varepsilon$ (i.e. $\varepsilon_l-\varepsilon_r$) and ε were calculated at the maximum concentration of the particular species obtained from potentiometric data. EPR spectra were recorded on a Bruker ESP 300E spectrometer at X-band frequency (9.3 GHz) at 120 K. The EPR parameters were calculated for the spectra obtained at the maximum concentration of the particular species for which well-resolved components were observed. The solutions for EPR measurements with ethylene glycol (water–glycol, 2:1, v/v) were prepared to ensure good glass formation in frozen solutions. Copper(II) stock solution was prepared from $Cu(NO_3)_2\cdot6H_2O$. The metal concentration in all spectroscopic measurements was adjusted to 1×10^{-3} M and the metal-to-ligand molar ratio was 1:1.1. For the water solution containing copper(II) ions and the peptide fragments: (1–28**H**) and (1–28**M**), the precipitation in pH range 4.5–8 was observed.

It was shown that the (1–28) fragment of β-amyloid peptide produces insoluble β-pleated sheet structures in vitro, similar to the β-pleated sheet structures of β peptide in amyloid deposits in vivo. For peptide solutions in the millimolar range (conditions of spectroscopic studies), in aqueous solution at pH 1–4 the (1–28) peptide adopts a monomeric random coil structure, and at pH 4–7 the peptide rapidly precipitates from solution as an oligomeric β-sheet structure, analogous to amyloid deposition in vivo [34]. The NMR solution structure at low pH [34,35] and CD and NMR evidence of an α-helix to β-sheet transition at mid-range pH [36] are in good agreement with the molecular dynamics simulations [37]. It is suggested that hydrophobic residues within the His^{13}–His^{14}–Gln^{15}–Lys^{16}–Leu^{17}–Val^{18}–Phe^{19}–Phe^{20} section are likewise critical to the formation of stable amyloid-like deposits [34]. β-peptides with Phe^{19}, Phe^{20}, or Lys^{16} substituted do not form amyloid filaments in vitro [38], demonstrating that this region is important for stabilization of the β-pleated sheet in amyloid deposits. For the solutions with high ionic strength (conditions of potentiometric studies) only monomeric β-peptide structures were observed [38].

3. Results and discussion

3.1. Protonation constants

Protonation constants (log β, log K values) for the peptides studied and comparable ligands are given in Tables 1 and 2. The first protonation constant, log β_{HL}, for the peptides studied is the ε-amino group of the Lys

Table 1
Protonation constants for 1–16**H**, 1–16**M**, 1–28**H** and 1–28**M** fragments of β-amyloid peptide and comparable peptides at 298 K and I=0.10 M (KNO_3)

Peptide	Log β											
	HL	H_2L	H_3L	H_4L	H_5L	H_6L	H_7L	H_8L	H_9L	$H_{10}L$		
1–16**H**	9.96±0.01	17.89±0.01	24.84±0.01	31.38±0.01	37.10±0.01	41.47±0.01	45.37±0.01	48.52±0.01	51.18±0.01			
1–28**H**	10.46±0.01	20.28±0.01	28.32±0.01	35.53±0.01	42.03±0.01	47.59±0.01	52.04±0.01	55.91±0.01	59.50±0.01	62.53±0.01		
1–16**M**	10.21±0.01	18.19±0.01	25.06±0.01	31.21±0.01	35.84±0.01	39.76±0.01	43.10±0.01	45.18±0.02				
1–28**M**	9.64±0.01	17.39±0.02	24.29±0.02	30.42±0.02	35.42±0.03	39.90±0.03	44.01±0.04	47.79±0.04	51.00±0.05	54.09±0.03		
1–10**H**[a]	9.87	17.59	24.02	28.35	31.86	34.54						
1–10**M**[a]	7.88	14.55	19.04	22.70	25.49							
	Log K											
	NH_2-Lys	O-Tyr	NH_2	N-Im	N-Im	N-Im	CO_2^-	CO_2^-	CO_2^-	CO_2^-	CO_2^-	CO_2^-
1–16**H**		9.96	7.93	6.95	6.54	5.72	4.37	3.90	3.15	2.66		
1–28**H**	10.46	9.82	8.04	7.21	6.50	5.56	4.45	3.87	3.59	3.03		
1–16**M**	10.21		7.98		6.87	6.15	4.63	3.92	3.34	2.08		
1–28**M**	9.64		7.75		6.90	6.13	5.00	4.48	4.11	3.78	3.21	3.09
1–10**H**		9.87	7.72		6.43		4.33		3.51	2.68		
1–10**M**			7.88		6.67		4.49		3.66	2.79		

[a] Ref. [29].

Table 2
Protonation constants for Ac-1–16**H** and Ac-1–16**M** fragments of β-amyloid peptide and comparable peptides at 298 K and I=0.10 M (KNO_3)

Peptide	Log β								
	HL	H_2L	H_3L	H_4L	H_5L	H_6L	H_7L	H_8L	H_9L
Ac-1–16**H**	9.78±0.01	19.54±0.01	26.87±0.01	33.38±0.01	39.39±0.01	44.11±0.01	48.18±0.02	51.83±0.02	54.54±0.02
Ac-1–16**M**	10.19±0.01	17.21±0.01	23.45±0.01	28.23±0.01	32.29±0.01	35.87±0.02	38.25±0.04		
Ac-1–6**H**[a]	6.50	10.95	14.45						
Ac-11–16**H**[b]	10.39	17.21	23.15	27.07					
Ac-1–6**M**[a]	6.79	11.39	15.02						
Ac-11–16**M**[b]	10.19	16.45	20.49						
Ac-HGHG[c]	6.945	13.264	16.51						
	Log K								
	NH_2-Lys	O^--Tyr	N-Im	N-Im	N-Im	CO_2^-	CO_2^-	CO_2^-	CO_2^-
Ac-1–16**H**	9.78 or 9.76	9.78 or 9.76	7.33	6.51	6.01	4.72	4.07	3.65	2.71
Ac-1–16**M**	10.19			7.02	6.24	4.78	4.06	3.58	2.38
Ac-1–6**H**				6.50		4.45		3.50	
Ac-11–16**H**	10.39		6.82		5.94		3.92		
Ac-1–6**M**				6.79		4.60		3.63	
Ac-11–16**M**	10.19				6.26	4.04			
Ac-HGHG			6.945	6.319			3.246		

[a] Ref. [29].
[b] Ref. [30].
[c] Ref. [58].

residue. For the (1–16**M**), (1–28**H**), (1–28**M**), (Ac-1–16**H**) and (Ac-1–16**M**) peptide fragments, the protonation values of the ε-amino nitrogen of the lysine residue (log K=10.46–9.64) agree well with literature data (Tables 1 and 2) [39–41]. The (1–28) fragments of human and mouse β-amyloid peptide contain two lysine residues (K^{16} and K^{28}), however, in the measurable pH range (2.5–10.5) one protonation constant was only detected (Table 1). It is suggested that two lysine residues for the human (1–28) fragment are in different environments. The side chain of Lys 16 is solvent exposed, whereas the side chain of Lys 28 is solvent shielded and it is likely that ε-NH_3^+ of Lys 28 may participate in hydrogen bonds [34,42]. The protonation constant of one lysine residue (K^{16}), which is present in the (1–16**H**) peptide fragment was not detected in this pH range (Table 1). However, the presence of this protonation constant for the (Ac-1–16**H**) peptide may suggest the involvement of the amino group in the formation of the hydrogen bond with the lysine residue (K^{16}) and/or its influence on the secondary structure of the (1–16**H**) peptide fragment. The (1–16**H**), (1–28**H**) and (Ac-1–16**H**) peptide fragments have tyrosine residue (Tyr^{10}) in the peptide sequence and the stepwise protonation constant of the phenolate group of the Tyr side chain (log K=9.96–9.76) corresponds very well to that of the (1–10**H**) fragment (Tables 1 and 2) [29]. For the (1–16) and (1–28) fragments with a free N-terminal amino group, the protonation constants log K=8.04–7.75 correspond very well to protonation of the N-terminal amino nitrogen (Table 1) and these values are comparable with those for the (1–10) fragments [29]. The (1–16**M**), (1–28**M**) and (Ac-1–16**M**) peptide fragments have two protonation constants, and the (1–16**H**), (1–28**H**) and (Ac-1–16**H**) fragments three protonation constants which correspond to protonation of the imidazole nitrogen of the histidine residues (His^6, His^{14} and His^6, His^{13}, His^{14}, respectively) (Tables 1 and 2). The values (log K=7.33–5.56) are close to those expected for comparable peptides (Tables 1 and 2) [43,44]. The protonation constants of carboxyl groups of the Asp and Glu amino acid residues (log K=5.00–2.08) in all ligands studied are close to those of peptides containing aspartic and/or glutamic acids in their peptide sequence (Tables 1 and 2) [45]. The (1–28) fragments of human and mouse β-amyloid peptide contain six carboxylate groups (three of Glu and three of Asp residues), however, for the (1–28**H**) fragment two protonation constants of these groups were not detected in the measurable pH range (2.5–10.5). Different values for protonation constants of carboxylate groups for the (1–28**H**) and (1–28**M**) fragments (Table 1) may suggest different formations of hydrogen bonds and/or different secondary structure of these peptides (likely because of three different substitutions in positions 5, 10 and 13). The carboxylate residues ionize above pH 4 and it is suggested that the unfavorable electrostatic repulsions among the ionized carboxylates may promote α-helix disruption for the human (1–28) fragment [34].

Potentiometry detects a range of Cu^{2+} complexes with the formation constants reported in Tables 3 and 4 and Table 5 contains the values of log K*, the protonation corrected stability constants which are useful to compare the ability of various ligands to bind a metal ion [46,47]. Spectroscopic properties of major complexes are collected in Tables 6 and 7.

Table 3
Stability constants of copper(II) complexes of Ac-1–16**H** and Ac-1–16**M** fragments of β-amyloid peptide and comparable peptides at 298 K and I=0.10 M (KNO_3)

Peptide	Log β								
	CuH_4L	CuH_3L	CuH_2L	CuHL	CuL	$CuH_{-1}L$	$CuH_{-2}L$	$CuH_{-3}L$	$CuH_{-4}L$
Ac-1–16**H**	38.08±0.01	33.16±0.01	27.19±0.01	19.70±0.01	11.86±0.01	2.96±0.01	−6.79±0.01	−16.87±0.01	
Ac-1–16**M**		26.55±0.04	22.32±0.01	17.10±0.01	10.15±0.02	3.44±0.01	−4.16±0.01	−13.24±0.01	−24.08±0.02
Ac-1–6**H**[a]					4.49		−8.14	−16.16	
Ac-11–16**H**[b]			21.03	16.21	10.18	2.86	−6.31	−16.72	
Ac-1–6**M**[a]					4.95	−2.23	−8.48	−15.91	
Ac-11–16**M**[b]				14.01		1.93	−6.66	−16.83	
Ac-HGHG[c]				11.04	6.49	0.40	−6.13	−16.41	
Calculated deprotonation constants for histidine and amide protons (pK) in Cu(II) complexes	pK(His)	pK(His)	pK_1(amide)	pK_2(amide)	pK_3(amide)				
Ac-1–16**H**	4.92	5.97	7.49	7.84	8.90				
Ac-1–16**M**	5.22		6.95	6.71	7.60				
Ac-1–6**H**					8.02				
Ac-11–16**H**	4.82		6.03	7.32	9.17				
Ac-1–6**M**			7.18	6.25	7.43				
Ac-11–16**M**					8.59				
Ac-HGHG	4.55		6.09	6.53	10.28				

[a] Ref. [29].
[b] Ref. [30].
[c] Ref. [58].

*3.2. Cu(II) complexes with the (Ac-1–16**H**) and (Ac-1–16**M**) fragments of β-amyloid peptide*

Eight metal complex species can be fitted to the experimental titration curves obtained for the Cu(II)–(Ac-1–16**H**) system: CuH_4L, CuH_3L, CuH_2L, CuHL, CuL, $CuH_{-1}L$, $CuH_{-2}L$ and $CuH_{-3}L$ (Table 3, Fig. 1). The coordination starts via the imidazole nitrogen and leads to the formation of CuH_4L, as is expected for the N-blocked peptides containing the histidine residues [39,48–50]. With increasing pH above 4.5 the CuH_3L and CuH_2L complexes are formed with pK values for deprotonations of the CuH_4L and CuH_3L species ($CuH_4L \rightarrow CuH_3L \rightarrow CuH_2L$) equal to 4.92 and 5.97, respectively (Table 3). The formation of CuH_3L and CuH_2L is accompanied by a significant blue shift of the absorption band suggesting coordination of the additional nitrogen donors (Table 6). The EPR parameters for the CuH_3L and CuH_2L complex-

Table 4
Stability constants of copper(II) complexes of 1–16**H**, 1–28**H**, 1–16**M** and 1–28**M** fragments of β-amyloid peptide and comparable peptides at 298 K and I=0.10 M (KNO_3)

Peptide	Log β								
	CuH_5L	CuH_4L	CuH_3L	CuH_2L	CuHL	CuL	$CuH_{-1}L$	$CuH_{-2}L$	$CuH_{-3}L$
1–16**H**		35.99±0.01	31.49±0.01	26.22±0.01	20.12±0.01	12.63±0.01	4.10±0.01	−5.21±0.01	−15.28±0.01
1–28**H**	47.11±0.02	42.40±0.02	37.82±0.01	31.58±0.01	23.98±0.01	15.50±0.02	6.48±0.02	−3.29±0.02	−13.53±0.02
1–16**M**			30.08±0.03	25.33±0.01	19.55±0.02	12.98±0.02	3.95±0.03	−5.42±0.02	−15.77±0.02
1–28**M**		34.72±0.02	29.93±0.02	24.97±0.01	19.10±0.01	12.27±0.01	3.52±0.02	−6.04±0.02	−15.75±0.02
1–10**H**[a]				23.15	18.11	12.02	3.60	−5.35	−15.48
1–10**M**[a]					13.61	8.32	3.21	−6.34	−15.43
Calculated deprotonation constants for histidine and amide protons (pK) in Cu(II) complexes	pK(His)	pK(His)	pK_1(amide)	pK_2(amide)	pK_3(amide)				
1–16**H**	4.50	5.27	7.49	8.53	9.31				
1–28**H**	4.71	4.58	7.60	8.48	9.02				
1–16**M**	4.75		5.78	9.03	9.37				
1–28**M**	4.96		5.87	8.75	9.56				
1–10**H**	5.04		6.09	8.42	8.95				
1–10**M**	5.29		5.11	9.55	9.09				

[a] Ref. [29].

Table 5
Calculated log K^* values for Cu(II) complexes with N-terminal fragments of human and mouse β-amyloid peptide 1–16, 1–28, Ac-1–16 and comparable ligands

Peptide/log K^*[a]	1N {NH_2, COO^-} or 1N {N_{Im}}	2N {NH_2, COO^-, N_{Im}}	3N {NH_2, COO^-, $2N_{Im}$}	3N {NH_2, COO^- or CO, N^-, N_{Im}}	4N {NH_2, $2N^-$, N_{Im}}	4N {N_{Im}, $3N^-$}	
1–16**H**	−1.11	−5.61	−10.88	−10.98	−19.51	−20.89	
1–28**H**	−0.48	−5.19	−9.77	−9.90	−18.38	−19.36	
1–16**M**	−1.13	−5.88		−11.66	−20.39	−21.78	
1–28**M**	−0.49	−5.45		−11.32	−20.00	−21.81	
1–10**H**	−0.87	−5.91		−12.00	−20.42		
1–10**M**	−0.94	−6.23		−11.34	−20.89		
	1N {N_{Im}}	2N {$2N_{Im}$}	2N {N_{Im}, N^-}	3N {$3N_{Im}$}	3N {$2N_{Im}$, N^-}	3N {N_{Im}, $2N^-$}	4N {N_{Im}, $3N^-$}
Ac-1–16**H**	−1.31	−6.23	−5.85	−12.20	−13.18	−13.69	−22.59
Ac-1–16**M**	−1.13	−6.35	−6.28		−13.30	−13.77	−21.37
Ac-11–16**H**	−2.12	−6.94	−6.15		−12.97	−13.47	−22.64
Ac-1–6**H**	−2.01					−14.64	−22.66
Ac-11–16**M**	−2.44					−14.52	−23.11
Ac-1–6**M**	−1.84		−9.02			−15.27	−22.70
Ac-HGHG	−2.22	−6.77	−5.92		−12.86	−12.45	−22.73

[a] log K^*=log $\beta(CuH_jL)$−log $\beta(H_nL)$ (where the index j corresponds to the number of the protons in the coordinated ligand to metal ion and n corresponds to the number of protons coordinated to ligand).

Table 6
Spectroscopic data for copper(II) complexes of Ac-1–16**H** and Ac-1–16**M** fragments

Ligand/species	UV–Vis		CD		EPR	
	λ (nm)	ε (M^{-1} cm^{-1})	λ (nm)	$\Delta\varepsilon$ (M^{-1} cm^{-1})	A_{II} (G)	g_{II}
Ac-1–16**H**						
CuH_3L {N_{Im}, N_{Im}}	644[a]	90			156	2.310
CuH_2L {N_{Im}, N_{Im}, N_{Im}}	617[a]	117			160	2.286
CuHL {N_{Im}, N^-, N_{Im}}	593[a]	130	556[a]	+0.290	182	2.256
			358[b]	−0.190		
			260[c]	+3.138		
CuL {N_{Im}, $2N^-$}	582[a]	121	552[a]	+0.271	160	2.235
			356[b]	−0.409		
			257[c]	+6.204		
$CuH_{-1}L$, $CuH_{-2}L$, $CuH_{-3}L$ {N_{Im}, $3N^-$}	522[a]	147	648[a]	+1.259	192	2.189
			500[a]	−1.259		
			357[b]	−0.605		
			316[d]	+1.459		
			268[c]	+8.001		
Ac-1–16**M**						
CuH_2L {N_{Im}}	704[a]	26			151	2.323
CuHL {N_{Im}, N_{Im}}	652[a]	54	334[b]	−0.040	162	2.302
			262[c]	+0.693		
$CuH_{-1}L$ {N_{Im}, $2N^-$}	598[a]	96	530[a]	+0.077	172	2.233
			358[b]	−0.675		
			318sh[d]	+0.307		
			266[c]	+3.830		
$CuH_{-2}L$ {N_{Im}, $3N^-$}	528[a]	110	614[a]	+0.899	194	2.193
			488[a]	−0.701		
			360[b]	−0.583		
			316[d]	+1.262		
$CuH_{-3}L$ {N_{Im}, $3N^-$}	523[a]	120	608[a]	+1.372	194	2.191
			491[a]	−1.221		
			360[b]	−0.247		
			318[d]	+1.780		
			270[c]	+2.631		

[a] d–d transition.
[b] N_{Im}→Cu(II) charge transfer transition.
[c] N_{Im} π_2→Cu(II) charge transfer transition.
[d] N^-(amide)→Cu(II) charge transfer transition.

Table 7
Spectroscopic data for copper(II) complexes of 1–16**H**, 1–28**H**, 1–16**M** and 1–28**M** fragments

Ligand/species	UV–Vis		CD		EPR	
	λ (nm)	ε (M^{-1} cm^{-1})	λ (nm)	$\Delta\varepsilon$ (M^{-1} cm^{-1})	A_{II} (G)	g_{II}
1–16**H**						
CuH_3L {NH_2, COO^-, N_{Im}}	649[a]	75			147	2.286
CuH_2L, CuHL {NH_2, COO^-, $2N_{Im}$}	615[a]	120			175	2.262
CuL {NH_2, N^-, CO, N_{Im}}	606[a]	126	576[a]	−0.267	156	2.229
			315[c]	+0.467		
			268[d]	+0.207		
$CuH_{-1}L$ {NH_2, $2N^-$, N_{Im}}	574[a]	118	554[a]	−0.377	182	2.203
			371[b]	−0.046		
			316[c]	+0.609		
			286[e]	−0.025		
			266[d]	+0.452		
$CuH_{-2}L$, $CuH_{-3}L$ {N_{Im}, $3N^-$}	511[a]	174	656[a]	+0.219	196	2.190
			508[a]	−1.181		
			358[b]	−0.092		
			316[c]	+0.784		
			265[d]	+2.555		
1–28**H**						
$CuH_{-1}L$, $CuH_{-2}L$, $CuH_{-3}L$ {N_{Im}, $3N^-$}	518[a]	162	646[a]	+1.098	202	2.183
			501[a]	−1.808		
			357[b]	−0.483		
			318[c]	+1.398		
			277[d]	+3.957		
1–16**M**						
CuH_3L {NH_2, COO^-} or {N_{Im}}					153	2.326
CuH_2L {NH_2, COO^-, N_{Im}}	645[a]	65			139	2.297
CuHL {NH_2, COO^-, N^-, N_{Im}}	610[a]	106	676[a]	−0.342	158	2.228
			540[a]	+0.165		
			348[b]	−0.218		
			304sh[c]	+0.356		
			269[d]	+1.322		
CuL {NH_2, COO^-, N^-, N_{Im}}	613[a]	113	677[a]	−0.331	157	2.229
			542[a]	+0.263		
			350[b]	−0.384		
			307sh[c]	+0.485		
			276[d]	+1.775		
$CuH_{-2}L$, $CuH_{-3}L$ {N_{Im}, $3N^-$}	512[a]	157	628[a]	+0.504	204	2.177
			496[a]	−1.507		
			361[b]	−0.185		
			314[c]	+1.676		
1–28**M**						
$CuH_{-2}L$, $CuH_{-3}L$ {N_{Im}, $3N^-$}	512[a]	195	631[a]	+0.176	202	2.184
			505[a]	−1.213		
			314[c]	+0.949		

[a] d–d transition.
[b] N_{Im}→Cu(II) transition.
[c] N^-(amide)→Cu(II) charge transfer transition.
[d] N_{Im} π_2→Cu(II) charge transfer transition.
[e] NH_2→Cu(II) charge transfer transition.

es, A_{II}=156 G, g_{II}=2.310 and A_{II}=160 G, g_{II}=2.286, respectively, are consistent with 2N {N_{Im}, N_{Im}} and 3N {N_{Im}, N_{Im}, N_{Im}} coordination of the peptide to copper(II) ions (Table 6) [30,50,51]. The A_{II} values for these complexes are lower than those for the imidazole complexes [51], however, it may reflect deformation of the complex plane expected when macrochelate rings are formed [29,52]. The CuH_2L complex with 3N {N_{Im}, N_{Im}, N_{Im}} coordination mode is present in a wide pH range of solution including physiological pH (Fig. 1). The CuHL, CuL and $CuH_{-1}L$ complexes are formed by sequential deprotonation and coordination of peptide nitrogens. The data show that the first pK_1(amide) value (deprotonation and coordination of amide nitrogen) for the N-blocked peptide coordinated to copper(II) ion by the imidazole nitrogen, is significantly higher than that of peptides coordinated by N-terminal amino group e.g. tetraglycine (pK_1(amide)=5.56) [30,48,49]. It could be explained by

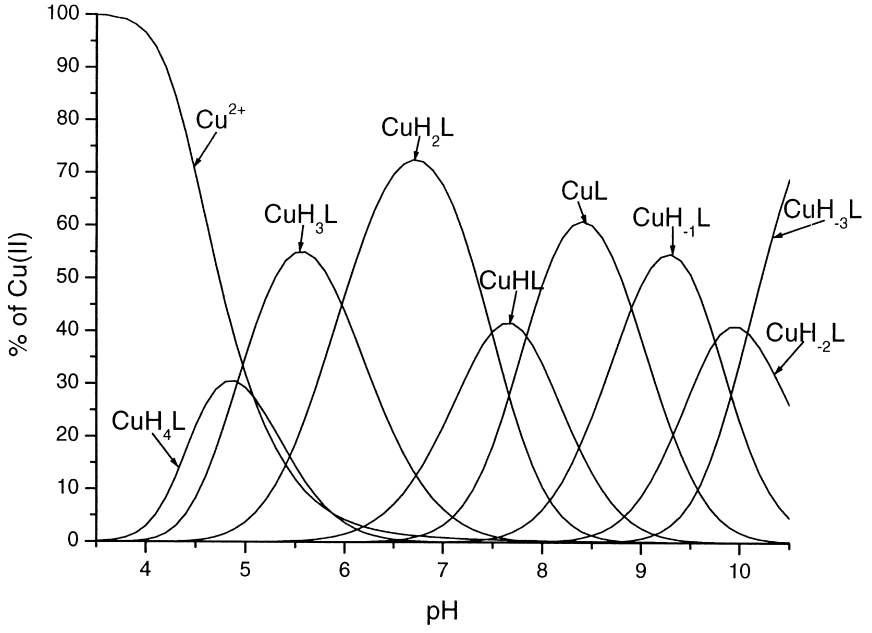

Fig. 1. Concentration distribution of the complexes formed in the Cu(II)–Ac-1–16**H** system as a function of pH. Cu(II)-to-peptide molar ratio 1:1, [Cu(II)]=0.001 M.

assuming that the metal bonding to the carbonyl group {NH_2, CO} for the peptides coordinated by amino group produces an electron-attracting effect, which favours the deprotonation and coordination of the adjacent amide nitrogen. The pK_1(amide) value (7.49, Table 3) for the (Ac-1–16**H**) peptide is about 1.5 orders of magnitude higher compared to that of (Ac-11–16**H**) fragment while the pK_2(amide) and pK_3(amide) values are comparable to each other. The parameters of the UV–Vis, CD and EPR spectra obtained for the CuHL, CuL and $CuH_{-1}L$ species (Fig. 1, Table 6) are comparable to the CuL, $CuH_{-1}L$ and $CuH_{-2}L$ complexes of the (Ac-11–16**H**) fragment of β-amyloid peptide [30], respectively, and to the complexes formed by the (Ac-11–20**H**) and (Ac-11–28**H**) fragments [31]. The coordination mode of copper(II) ion in these complexes is similar, i.e. the Cu^{2+} ion coordinates via {N_{Im}, N^-, N_{Im}}=3N, {N_{Im}, $2N^-$}=3N and {N_{Im}, $3N^-$}= 4N donor sets (N^- corresponds to a deprotonated amide nitrogen). The molar extinction coefficients (absorption spectra, Table 6) for the (Ac-1–16**H**) complexes are higher compared to those of the (Ac-11–16**H**) [30] suggesting that the complexes of the (Ac-1–16**H**) fragment assume a distorted geometry with a significant deviation from planarity. The parameters of UV–Vis, CD and EPR spectra are not altered in pH 9–10.5 suggesting for the $CuH_{-2}L$ and $CuH_{-3}L$ complexes the same 4N {N_{Im}, $3N^-$} coordination mode. Moreover, the protonation constants of the $CuH_{-3}L$ and $CuH_{-2}L$ complexes (10.08, 9.75, respectively, Table 3) are comparable to those for protonations of the Lys and Tyr residues in the metal-free ligand (9.78, 9.76, Table 2). In the spectroscopic studies around 400 nm there was a complete absence of the characteristic charge-transfer band $O^-_{Tyr}\rightarrow Cu^{2+}$ suggesting the lack of interaction of the phenolate –OH group of the Tyr residue with copper(II) ions in the whole pH range [53,54]. The log K^* values for the CuH_4L and CuH_3L complexes are 0.7–0.8 orders of magnitude higher for the (Ac-1–16**H**) than those of (Ac-11–16**H**) peptide (Table 5). This stabilization of the 1N {N_{Im}} and 2N {N_{Im}, N_{Im}} complexes for the (Ac-11–28**H**) fragment containing 18 amino acid residues was observed [31]. Values of log K^* for complexes with 3N and 4N coordination for the (Ac-1–16**H**) fragment of β-amyloid peptide are comparable with those of the (Ac-11–16**H**) fragment (Table 5).

Calculations based on the potentiometric data have revealed in the Cu(II)–Ac-1–16**M** system the presence of the following species: CuH_3L, CuH_2L, CuHL, CuL, $CuH_{-1}L$, $CuH_{-2}L$, $CuH_{-3}L$ and $CuH_{-4}L$ (Table 3, Fig. 2). The CuH_3L and CuH_2L species correspond to the 1N {N_{Im}} complexes. The pK value for deprotonation of the CuH_3L complex is equal to 4.23 and may suggest deprotonation of the carboxylate group in the complex (Table 3). The EPR parameters A_{II}=151 G, g_{II}=2.323 and d–d transition at 704 nm (absorption spectrum) for the CuH_2L species clearly indicate the 1N complex with one nitrogen atom from imidazole of histidine bound to a metal ion [29–31,51,55,56]. The deprotonation of the CuH_2L complex with pK value 5.22 (Table 3), the presence in CD spectrum of $N_{Im}\rightarrow Cu^{2+}$ charge transfer transition at 334 nm [57] and EPR parameters A_{II}=162 G, g_{II}=2.302 (Table 6) may suggest for the CuHL complex the 2N {N_{Im}, N_{Im}} coordination mode [51,58]. Three other species formed by the (Ac-1–16**M**) fragment, i.e. CuL, $CuH_{-1}L$ and $CuH_{-2}L$ are the complexes with sequential deprotona-

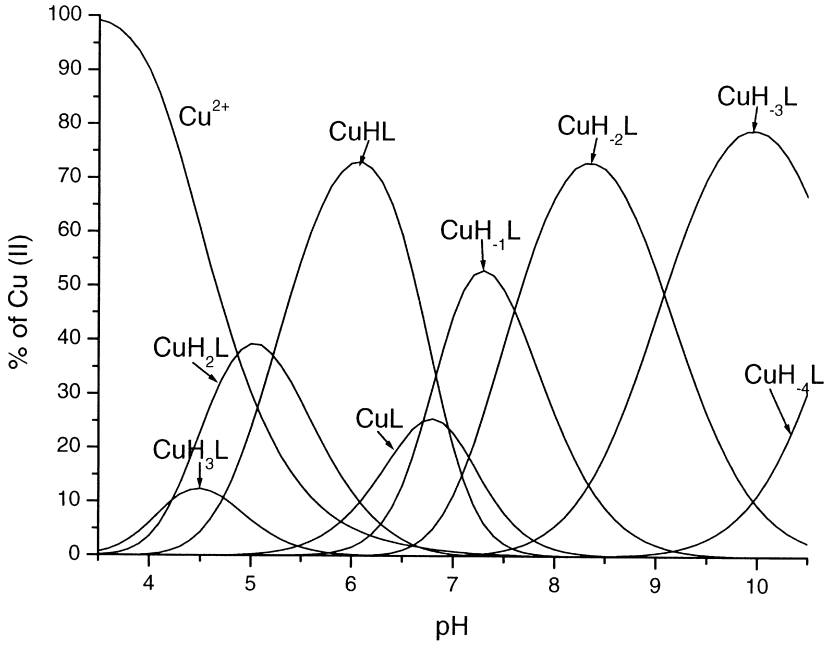

Fig. 2. Concentration distribution of the complexes formed in the Cu(II)–Ac-1–16**M** system as a function of pH. Details as in Fig. 1.

tion and coordination of the amide nitrogens. The $CuH_{-1}L$ complex is shown by absorption, CD and EPR spectroscopy to involve 3N coordination with $\{N_{Im}, 2N^-\}$ bonding mode (Table 6) [29–31,39,56]. The low value of $\Delta\varepsilon$ for d–d transition in the CD spectrum (+0.077, Table 6) may suggest, beside the amide and the imidazole nitrogens of His^6, the involvement of the amide nitrogen of Gly^5 in the formation of the chelate rings. The CD spectra obtained for the $CuH_{-2}L$ species of the (Ac-1–16**M**) peptide with the $\{N_{Im}, 3N^-\}$ coordination mode (Table 6) are closer to those of the (Ac-1–6**M**) [29] suggesting the coordination of the imidazole and amide nitrogens of His^6 and the amide nitrogens of Gly^5 and Phe^4 to copper(II) ions. Above pH 8 (Fig. 2) the deprotonations of the $CuH_{-2}L$ and $CuH_{-3}L$ species take place (pK values 9.08 and 10.84, respectively). The deprotonation of the $CuH_{-2}L$ complex may correspond to the deprotonation of the Lys (K^{16}) residue in the complex and the relatively low value compared to that in metal-free ligand (10.19, Table 2) may suggest some involvement of Lys^{16} side chain in the interaction with metal ion. The log K* values for the (Ac-1–16**M**) complexes are comparable to those of the (Ac-1–16**H**) with similar coordination mode except the $CuH_{-2}L$ complex with 4N $\{N_{Im}, 3N^-\}$ bonding mode (Table 5). The stabilization of the $CuH_{-2}L$ complex by about one order of magnitude compared to those of the (Ac-1–6**M**) and (Ac-1–16**H**) peptides may result from the interaction of the Lys^{16} residue with metal ion.

The (Ac-1–16**H**) and (Ac-1–16**M**) fragments of β-amyloid peptide form different complexes. The human fragment in a wide pH range (5–8) forms with copper(II) ions the 3N $\{N^6_{Im}, N^{13}_{Im}, N^{14}_{Im}\}$ complex while in 8.5–10.5 pH range the formation of the 4N $\{N_{Im}, 3N^-\}$ complex is proposed. The (Ac-1–16**M**) fragment containing two histidine residues (His^6 and His^{14}) forms the 2N $\{N^6_{Im}, N^{14}_{Im}\}$ complex in pH range 5–7, whereas in high pH 7.5–10.5 the 4N $\{N^6_{Im}, 3N^-\}$ complex is suggested.

*3.3. Cu(II) complexes with the (1–16**H**), (1–28**H**), (1–16**M**) and (1–28**M**) fragments of β-amyloid peptide*

According to potentiometric and spectroscopic results, the mouse fragments of β-amyloid peptide (1–16**M**), (1–28**M**) form with Cu^{2+} ions the CuH_3L, CuH_2L, CuHL, CuL, $CuH_{-1}L$, $CuH_{-2}L$ and $CuH_{-3}L$ species (Table 4, Fig. 3). The (1–16**M**) and (1–28**M**) fragments contain in the amino acid sequence the same donor sets and the potentiometric and spectroscopic results suggest the formation of the complexes with similar coordination modes (Tables 4, 5 and 7, Fig. 3). For the (1–28**M**) fragment the CuH_4L complex was also detected, however, the pK value for deprotonation of the CuH_4L complex (4.79, Table 4) may correspond to the deprotonation of the carboxylate group in the complex. For the CuH_3L complex of the (1–16**M**) peptide the EPR parameters A_{II}=153 G, g_{II}= 2.326 are consistent with 1N $\{N_{Im}\}$ or $\{NH_2, COO^-$ of $Asp^1\}$ coordination (Table 7) [29–31]. The low value of pK for the deprotonation of the CuH_3L complex (4.75; 4.96 for both peptides, Table 4) corresponds very well to the deprotonation and coordination of the amine or imidazole nitrogens [52]. The parameters of UV–Vis and EPR spectra for the CuH_2L complex are similar to those of the (1–6**M**) peptide suggesting the 2N $\{NH_2, COO^-, N_{Im}\}$ coordination mode with the existence of a macrochelate in the molecule (Table 7) [29]. With increasing pH, CuHL and CuL complexes are formed (Fig. 3). The parameters of

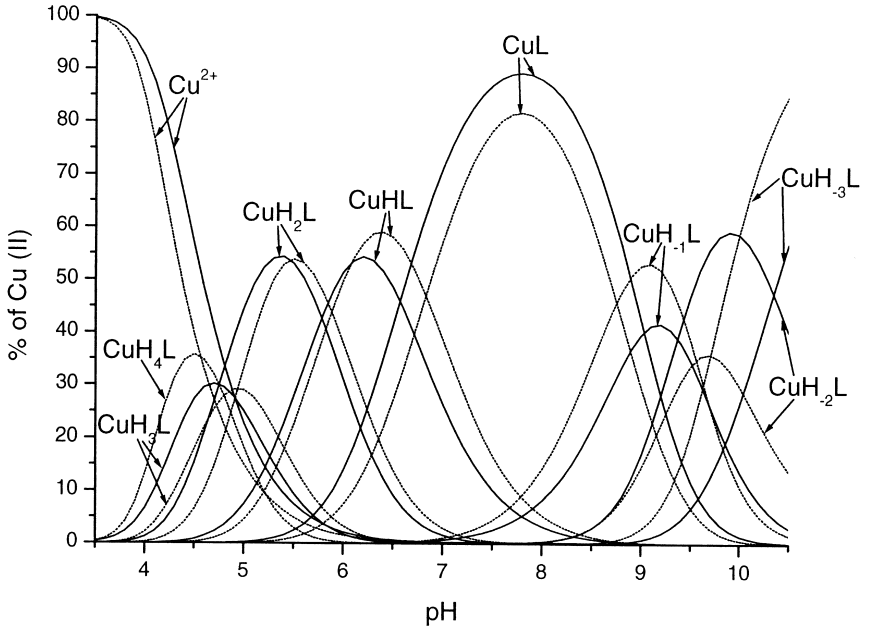

Fig. 3. Concentration distribution of the complexes formed in the Cu(II)–1–16**M** (solid lines) and 1–28**M** (dotted lines) systems as a function of pH. Details as in Fig. 1.

UV–Vis, CD and EPR spectra for these complexes are similar to each other and are consistent with {NH_2, COO^-, N^-, N_{Im}} bonding mode as was suggested for the (1–10**M**) fragment (Table 7) [29]. Moreover, the protonation constant of the CuL complex (6.57; 6.83 for both peptides) is comparable to that for protonation of the His residue in the metal-free ligand supporting the involvement of only one imidazole nitrogen in the interaction with copper(II) ion (Tables 1 and 4). Different signs of Cotton effects for d–d transitions for the CuHL and CuL complexes of the (1–16**M**) peptide compared to those of the (1–10**M**) peptide may suggest the involvement of the His^{14} residue in the coordination of metal ion. The complex with 3N {NH_2, COO^-, N^-, N_{Im}} coordination mode is present in the solution in a wide pH range including the physiological pH (Fig. 3). The two other deprotonations leading to $CuH_{-1}L$ and $CuH_{-2}L$ species with pK of 9.03 and 9.37 for the (1–16**M**) peptide (8.75 and 9.56 for the 1–28**M**, Table 4) can be assigned to deprotonation and coordination of the second and third amide nitrogens. The absorption band of the d–d transition at 512 nm, the EPR parameters A_{II}=202–204 G, g_{II}=2.177–2.184 and the parameters of CD spectra for the $CuH_{-2}L$ complex of both peptides strongly support the 4N {N_{Im}, $3N^-$} bonding mode (Table 7) [29–31]. The high values of pK_2(amide) for the (1–10**M**), (1–16**M**) and (1–28**M**) fragments (9.55, 9.03, 8.75, respectively, Table 4) compared to that of tetraalanine amide (7.74) [59] may strongly indicate that the formation of the 4N {NH_2, $2N^-$, N_{Im}} species from the 3N {NH_2, COO^-, N^-, N_{Im}} complex requires a reorganization of the donor set and/or structure around the metal ion bonding site. The next deprotonation (resulting in the $CuH_{-3}L$ species) has no effect on the structure of the complex formed, as seen from the CD, EPR and UV–Vis measurements (Table 7). It must in fact be due to deprotonation of the non-coordinated ε-amino group of the lysine residue. The protonation constant of the $CuH_{-3}L$ complex for the (1–16**M**) and (1–28**M**) peptides (10.35, 9.71, respectively) corresponds very well to that in free ligand (10.21, 9.64, respectively, Tables 1 and 4). The log K* values for the complexes of the (1–16**M**) and (1–28**M**) peptides are comparable to those of the (1–10**M**) fragment except the $CuH_{-2}L$ complex with the 4N {N_{Im}, $3N^-$} coordination mode. The log K* value for this complex is comparable to that of the (Ac-1–16**M**) peptide (Table 5).

From potentiometric data calculations, eight and nine monomeric complexes are found for the Cu(II)–1–16**H** and Cu(II)–1–28**H** systems, respectively (Table 4, Fig. 4). For the (1–28**H**) peptide the protonation constant of the Lys residue was detected, therefore, from the point of view of Cu(II) bonding, the 1N complex with (1–16**H**) fragment will be the CuH_4L species while with the (1–28**H**) peptide it will be the CuH_5L complex. Likewise the 2N species will be CuH_3L and CuH_4L, respectively, with corresponding relationships for the next (3N, 4N) complexes. The coordination of metal ion starts at pH around 3.5 with 1N {NH_2, COO^- of Asp^1 residue} or {N_{Im}} bonding mode (Fig. 4) [29–31]. The log K* value for the (1–16**H**) peptide is comparable to that of the (Ac-1–16**H**) fragment suggesting 1N {N_{Im}} coordination mode (Table 5). The low pK values for the deprotonation reactions $CuH_4L \rightarrow CuH_3L + H^+$ and $CuH_3L \rightarrow CuH_2L + H^+$ (4.5, 5.27 for the 1–16**H** and 4.71, 4.58 for the 1–28**H**, Table 4) may suggest the sequential deprotonation and coordination

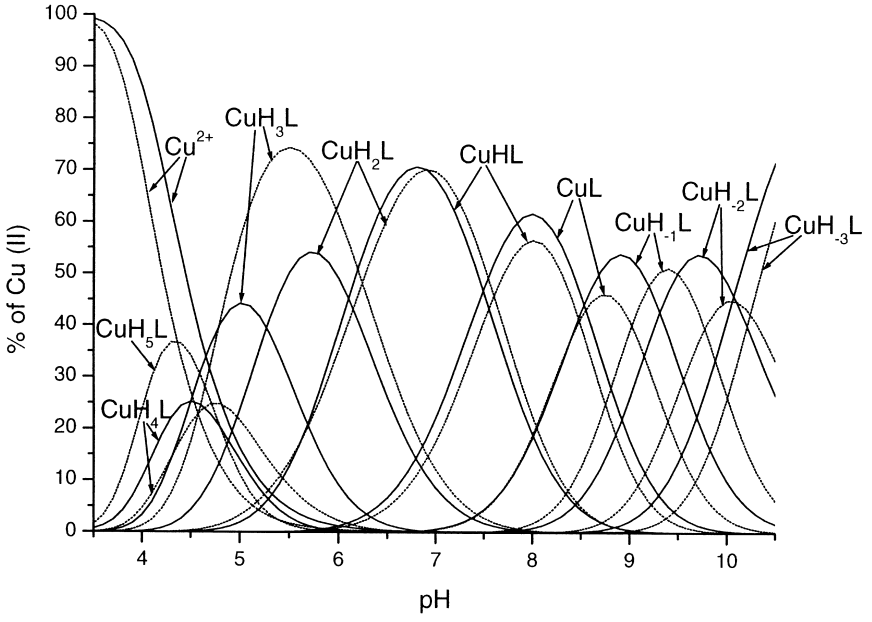

Fig. 4. Concentration distribution of the complexes formed in the Cu(II)–1–16**H** (solid lines) and 1–28**H** (dotted lines) systems as a function of pH. Details as in Fig. 1.

of the amine or imidazole nitrogens [52]. The EPR parameters A_{II}=175 G, g_{II}=2.262 and the absorption band of the d–d transition at 615 nm for the CuH_2L and CuHL complexes of the (1–16**H**) peptide strongly suggest 3N $\{NH_2, COO^-, N_{Im}, N_{Im}\}$ bonding mode (Table 7). Moreover, the protonation constants of the CuHL and CuH_2L complexes for the (1–16**H**) and (1–28**H**) peptides (6.10, 6.24, respectively) are in good agreement to those for protonations of the histidine residue in the free ligand suggesting the involvement of two imidazole nitrogens likely His^{13} and His^{14} residues in the coordination. The deprotonation reactions $CuHL \rightarrow CuL \rightarrow CuH_{-1}L \rightarrow CuH_{-2}L$ for the (1–16**H**) fragment and $CuH_2L \rightarrow CuHL \rightarrow CuL \rightarrow CuH_{-1}L$ for the (1–28**H**) peptide with p*K* 7.49, 8.53, 9.31 and 7.60, 8.48, 9.02, respectively, can be assigned to the deprotonation and coordination of the sequential amide nitrogens (Table 4). The UV–Vis, CD and EPR spectra for the CuL complex of the (1–16**H**) peptide are similar to those of the (1–10**H**) fragment suggesting the same 3N $\{NH_2, N^-, CO, N_{Im}\}$ coordination mode (Table 7) [29]. For the $CuH_{-1}L$ species of the (1–16**H**) peptide the presence in the CD spectrum of the $N_{Im} \rightarrow Cu^{2+}$, $N^- \rightarrow Cu^{2+}$ and $NH_2 \rightarrow Cu^{2+}$ charge transfer transitions at 371, 316 and 286 nm, respectively, clearly indicate to involve 3N coordination with $\{NH_2, 2N^-, N_{Im}\}$ bonding mode (Table 7). The parameters of the EPR and UV–Vis spectra are also consistent with this coordination mode [29,52]. For the $CuH_{-2}L$ and $CuH_{-3}L$ species of the (1–16**H**) fragment and the $CuH_{-1}L$, $CuH_{-2}L$, $CuH_{-3}L$ complexes of the (1–28**H**) peptide the EPR, UV–Vis and CD spectra are similar to each other and are comparable to those of the (Ac-1–6**H**), (Ac-11–16**H**) and (Ac-1–16**H**) with 4N $\{N_{Im}, 3N^-\}$ coordination mode (Table 7) [29,30]. The phenolate-oxygen of the Tyr residue does not coordinate since there was a complete absence of the characteristic charge transfer band in the CD and absorption spectra at about 400 nm (Table 7) [53,54]. Values of log *K** for complexes of the (1–28**H**) peptide with 3N $\{NH_2, N^-, CO, N_{Im}\}$ and 4N $\{NH_2, 2N^-, N_{Im}\}$ coordination modes are higher by about two orders of magnitude compared to those of the (1–10**H**) fragment. The 4N $\{N_{Im}, 3N^-\}$ complex of the (1–28**H**) peptide is stabilized by about three orders of magnitude compared to those of the (Ac-1–6**H**), (Ac-11–16**H**) and (Ac-1–16**H**) fragments (Table 5). This stabilization may result from structural organization of a peptide in copper(II) complex [31].

4. Conclusions

The fragments of β-amyloid peptide studied here did not reduce copper(II) ions in accordance with the observation reported earlier [20]. The imidazole nitrogen of the histidine residue acts as an anchoring bonding site for the human and mouse fragments, (Ac-1–16**H**) and (Ac-1–16**M**). In a wide pH range, Cu^{2+} is bound to the (Ac-1–16**M**) peptide through imidazole nitrogens on both of its histidine residues (His^6, His^{14}), while, for the (Ac-1–16**H**) fragment the 3N complex with $\{N^6_{Im}, N^{13}_{Im}, N^{14}_{Im}\}$ coordination mode is formed. With increasing pH sequential amide nitrogens are also bound and at pH above 9, the major complex with the 4N $\{N_{Im}, 3N^-\}$ bonding site is present in solution. The potentiometric and spectroscopic results for the (1–16**M**), (1–16**H**), (1–28**M**), (1–28**H**), (Ac-1–16**M**) and (Ac-1–16**H**) clearly indicate that the acetylation of the

N-terminal amino group has a major influence on both the speciation and structures of the complexes formed. N-terminal amino group takes part in the coordination, although at pH above 9 the 4N $\{N_{Im}, 3N^-\}$ bonding mode is suggested. The (1–16**M**) fragment forms complexes with similar coordination modes to those of the (1–10**M**) peptide up to pH 9. Above pH 9 the 4N $\{N_{Im}, 3N^-\}$ complex is formed as in the case of the (Ac-1–16**M**) peptide. For the (1–16**H**) and (1–28**H**) fragments the presence of the His^{13}–His^{14} sequence changes the coordination mode of the peptide compared to the mouse peptide. In a wide pH range, including physiological pH, the 3N complex is formed with the $\{NH_2, COO^-, N_{Im}, N_{Im}\}$ bonding site, where likely two histidine residues of the His^{13}–His^{14} sequence are involved in the interaction with the copper(II) ions. The spectroscopic data strongly suggest the 4N $\{N_{Im}, 3N^-\}$ coordination mode of these fragments at pH above 9. Addition of the (17–28) sequence to the (1–16) fragments of human and mouse β-amyloid peptide does not change the coordination mode, and the stabilities of the complexes formed are higher for the (1–28**H**) peptide by about 0.5–1.5 orders of magnitude compared to those of the (1–16**H**) fragment. The potentiometric and spectroscopic data clearly indicate that the tyrosine residue in the tenth position of the human fragments does not take part in the coordination of the metal ion.

Acknowledgements

This work was supported by the Polish State Committee for Scientific Research (KBN 3 T09A 06918).

References

[1] G.G. Glenner, C.W. Wong, Biochem. Biophys. Res. 120 (1984) 885.
[2] C.L. Masters, G. Simms, N.A. Weinman, G. Multhaup, B.L. McDonald, K. Beyreuther, Proc. Natl. Acad. Sci. USA 82 (1985) 4245.
[3] T.E. Golde, S. Estus, L.H. Younkin, D.J. Selkoe, S.G. Younkin, Science 255 (1992) 728.
[4] S.S. Sisodia, Proc. Natl. Acad. Sci. USA 89 (1992) 6075.
[5] D.J. Selkoe, Neuron 6 (1991) 487.
[6] N.W. Kowall, M.F. Beal, J. Busciglio, L.K. Duffy, B.A. Yanker, Proc. Natl. Acad. Sci. USA 88 (1991) 7247.
[7] M. Shoji, T.E. Golde, J. Ghiso, T.T. Cheung, S. Estus, L.M. Schaffer, X.-D. Cai, D. McKay, R. Tintner, B. Frangione, S.G. Younkin, Science 258 (1992) 126.
[8] J. Busciglio, D.H. Gabuzda, P. Matsudaira, B.A. Yanker, Proc. Natl. Acad. Sci. USA 90 (1993) 2092.
[9] C.S. Atwood, X. Huang, R.D. Moir, R.E. Tanzi, A.I. Bush, Metal Ions Biol. Syst. 36 (1999) 309.
[10] H. Basun, L.G. Forssell, L. Wetterberg, B. Winblad, J. Neural Transm. Parkinson's Dis. Dementia Sect. 3 (1991) 231.
[11] D.A. Loeffler, P.A. Lewitt, P.L. Juneau, A.A. Sima, H.U. Nguyen, A.J. DeMaggio, C.M. Brickman, G.J. Brewer, R.D. Dick, M.D. Troyer, L. Kanaley, Brain Res. 738 (1996) 265.
[12] R.A. Cherny, J.T. Legg, C.A. McLean, D.P. Fairlie, X. Huang, C.S. Atwood, K. Beyreuther, R.E. Tanzi, C.L. Masters, A.I. Bush, J. Biol. Chem. 274 (1999) 23223.
[13] C.S. Atwood, R.D. Moir, X. Huang, R.C. Scarpa, N.M. Bacarra, D.M. Romano, M.A. Hartshorn, R.E. Tanzi, A.I. Bush, J. Biol. Chem. 273 (1998) 12817.
[14] X. Huang, C.S. Atwood, R.D. Moir, M.A. Hartshorn, J.P. Vonsattel, R.E. Tanzi, A.I. Bush, J. Biol. Chem. 272 (1997) 26464.
[15] D.W. Vaughan, A. Peters, J. Neuropathol. Exp. Neurol. 40 (1981) 472.
[16] B.D. Shivers, C. Hilbich, G. Multhaup, M. Salbaum, K. Beyreuther, P.H. Seeburg, EMBO J. 7 (1988) 1365.
[17] T. Dyrks, E. Dyrks, C.L. Masters, K. Beyreuther, FEBS Lett. 324 (1993) 231.
[18] L.J. Otvos, G.I. Szendrei, V.M. Lee, H.H. Mantsch, Eur. J. Biochem. 211 (1993) 249.
[19] E.M. Johnstone, M.O. Chaney, F.H. Norris, R. Pascual, S.P. Little, Mol. Brain Res. 10 (1991) 299.
[20] X. Huang, M.P. Cuajungco, C.S. Atwood, M.A. Hartshorn, J.D.A. Tyndall, G.R. Hanson, K.C. Stokes, M. Leopold, G. Multhaup, L.E. Goldstein, R.C. Scarpa, A.J. Saunders, J. Lim, R.D. Moir, Ch. Glabe, E.F. Bowden, C.L. Masters, D.P. Fairlie, R.E. Tanzi, A.I. Bush, J. Biol. Chem. 274 (1999) 37111.
[21] S.T. Liu, G. Howlett, C.J. Barrow, Biochemistry 38 (1999) 9373.
[22] D.-S. Yang, J. McLaurin, K. Qin, D. Westaway, P.E. Fraser, Eur. J. Biochem. 267 (2000) 6692.
[23] C.C. Curtain, F. Ali, J. Volitakis, R.A. Cherny, R.S. Norton, K. Beyreuther, C.J. Barrow, C.L. Masters, A.I. Bush, K.J. Barnham, J. Biol. Chem. 276 (2001) 20466.
[24] W. Bal, J. Lukszo, K.S. Kasprzak, Chem. Res. Toxicol. 9 (1996) 535.
[25] G. Xing, V.J. DeRose, Curr. Opin. Chem. Biol. Rev. 5 (2001) 196.
[26] M.A. Zoroddu, L. Schinocca, T. Kowalik-Jankowska, H. Kozlowski, K. Salnikow, M. Costa, Environ. Health Perspect. 110 (Suppl. 5) (2002) 719.
[27] W. Bal, J. Am. Chem. Soc. 118 (1996) 4727.
[28] P. Tsiveriotis, N. Hadjiliadis, Co-ord. Chem. Rev. 190–192 (1999) 171.
[29] T. Kowalik-Jankowska, M. Ruta-Dolejsz, K. Wisniewska, L. Łankiewicz, J. Inorg. Biochem. 86 (2001) 535.
[30] T. Kowalik-Jankowska, M. Ruta-Dolejsz, K. Wisniewska, L. Łankiewicz, H. Kozłowski, J. Chem. Soc. Dalton Trans. (2000) 4511.
[31] T. Kowalik-Jankowska, M. Ruta-Dolejsz, K. Wisniewska, L. Łankiewicz, J. Inorg. Biochem. 92 (2002) 1.
[32] H. Irving, M.G. Miles, L.D. Pettit, Anal. Chim. Acta 38 (1967) 475.
[33] P. Gans, A. Sabatini, A. Vacca, J. Chem. Soc. Dalton Trans. (1985) 1195.
[34] M.G. Zagorski, C.J. Barrow, Biochemistry 31 (1992) 5621.
[35] J. Talafous, K.J. Macinowski, G. Klopman, M.G. Zagorski, Biochemistry 33 (1994) 7788.
[36] C.J. Barrow, A. Yasuda, P.T.M. Kenny, M.G. Zagorski, J. Mol. Biol. 225 (1992) 1075.
[37] K. Kishenbaum, V. Daggett, Biochemistry 34 (1995) 7629.
[38] C. Hilbich, B. Kisters-Woike, J. Reed, C.L. Masters, K. Beyreuther, J. Mol. Biol. 218 (1991) 149.
[39] M.A. Zoroddu, T. Kowalik-Jankowska, H. Kozlowski, H. Molinari, K. Salnikow, L. Broday, M. Costa, Biochim. Biophys. Acta 1475 (2000) 163.
[40] T. Kowalik-Jankowska, M. Jasionowski, L. Lankiewicz, J. Inorg. Biochem. 76 (1999) 63.
[41] I. Sovago, T. Kiss, A. Gergely, Inorg. Chim. Acta 93 (1984) L53.
[42] L.G. Presta, G.D. Rose, Science 240 (1988) 1632.
[43] C.E. Livera, L.D. Pettit, M. Bataille, B. Perly, H. Kozlowski, B. Radomska, J. Chem. Soc. Dalton Trans. (1987) 661.
[44] W. Bal, M. Jezowska-Bojczuk, K. Kasprzak, Chem. Res. Toxicol. 10 (1997) 906.
[45] J.-F. Galey, B. Decock-Le Reverend, A. Lebkiri, L.D. Pettit, S.I. Pyburn, H. Kozlowski, J. Chem. Soc. Dalton Trans. (1991) 2281.

[46] W. Bal, M. Dyba, H. Kozłowski, Acta Biochim. Pol. 44 (1997) 467.
[47] H. Kozłowski, W. Bal, M. Dyba, T. Kowalik-Jankowska, Coord. Chem. Rev. 184 (1999) 319.
[48] D. Sanna, C.G. Agoston, I. Sovago, G. Micera, Polyhedron 20 (2001) 937.
[49] M.A. Zoroddu, M. Peana, T. Kowalik-Jankowska, H. Kozlowski, M. Costa, J. Chem. Soc. Dalton Trans. (2002) 458.
[50] M. Luczkowski, K. Wisniewska, L. Lankiewicz, H. Kozlowski, J. Chem. Soc. Dalton Trans. (2002) 2266.
[51] E. Chruscinska, G. Micera, A. Panzanelli, A. Dessi, J. Chem. Res. (S) (1997) 106.
[52] K. Varnagy, J. Szabo, I. Sovago, G. Malandrinos, N. Hadjiliadis, D. Sanna, G. Micera, J. Chem. Soc. Dalton Trans. (2000) 467.
[53] R. Prados, R.K. Boggess, R.B. Martin, R.C. Woodworth, Bioinorg. Chem. 4 (1975) 135.
[54] C. Livera, L.D. Pettit, M. Bataille, J. Krembel, W. Bal, H. Kozlowski, J. Chem. Soc. Dalton Trans. (1988) 1357.
[55] B. Decock-Le Reverend, F. Liman, C. Livera, L.D. Pettit, S. Pyburn, H. Kozlowski, J. Chem. Soc. Dalton Trans. (1988) 887.
[56] M.A. Zoroddu, T. Kowalik-Jankowska, H. Kozlowski, K. Salnikow, M. Costa, J. Inorg. Biochem. 84 (2001) 47.
[57] T.G. Fawcett, E.E. Bernarducci, K. Krogh-Jespersen, H.J. Schugar, J. Am. Chem. Soc. 102 (1980) 2598.
[58] M. Casolaro, M. Chelli, M. Ginanneschi, F. Laschi, L. Messori, M. Muniz-Miranda, A.M. Papini, T. Kowalik-Jankowska, H. Kozlowski, J. Inorg. Biochem. 89 (2002) 181.
[59] W. Bal, H. Kozlowski, G. Kupryszewski, Z. Mackiewicz, L.D. Pettit, R. Robbins, J. Inorg. Biochem. 52 (1993) 79.